AGU PUBLICATIONS

Geophysical Research Letters

RESEARCH LETTER
10.1002/2014GL061669

Key Points:
- Aerosol sulfate mass has decreased faster than organic mass in the SE U.S.
- Aerosol water mass has decreased due to decreasing sulfate/organic ratio
- Aerosol extinction and radiative forcing have changed due to composition changes

Supporting Information:
- Readme
- Text S1

Correspondence to:
R. A. Washenfelder,
rebecca.washenfelder@noaa.gov

Citation:
Attwood, A. R., et al. (2014), Trends in sulfate and organic aerosol mass in the Southeast U.S.: Impact on aerosol optical depth and radiative forcing, *Geophys. Res. Lett.*, *41*, 7701–7709, doi:10.1002/2014GL061669.

Received 5 SEP 2014
Accepted 17 OCT 2014
Accepted article online 21 OCT 2014
Published online 11 NOV 2014

Trends in sulfate and organic aerosol mass in the Southeast U.S.: Impact on aerosol optical depth and radiative forcing

A. R. Attwood[1,2], R. A. Washenfelder[1,2], C. A. Brock[1], W. Hu[2,3], K. Baumann[4], P. Campuzano-Jost[2,3], D. A. Day[2,3], E. S. Edgerton[4], D. M. Murphy[1], B. B. Palm[2,3], A. McComiskey[1,2], N. L. Wagner[1,2], S. S. de Sá[5], A. Ortega[2,6], S. T. Martin[5], J. L. Jimenez[2,3], and S. S. Brown[1]

[1]Chemical Sciences Division, Earth System Research Laboratory, National Oceanic and Atmospheric Administration, Boulder, Colorado, USA, [2]Cooperative Institute for Research in Environmental Sciences, University of Colorado Boulder, Boulder, Colorado, USA, [3]Department of Chemistry and Biochemistry, University of Colorado Boulder, Boulder, Colorado, USA, [4]Atmospheric Research and Analysis, Inc., Cary, North Carolina, USA, [5]School of Engineering and Applied Sciences, Harvard University, Cambridge, Massachusetts, USA, [6]Department of Atmospheric and Oceanic Sciences, University of Colorado Boulder, Boulder, Colorado, USA

Abstract Emissions of SO_2 in the United States have declined since the early 1990s, resulting in a decrease in aerosol sulfate mass in the Southeastern U.S. of $-4.5(\pm0.9)\%\ yr^{-1}$ between 1992 and 2013. Organic aerosol mass, the other major aerosol component in the Southeastern U.S., has decreased more slowly despite concurrent emission reductions in anthropogenic precursors. Summertime measurements in rural Alabama quantify the change in aerosol light extinction as a function of aerosol composition and relative humidity. Application of this relationship to composition data from 2001 to 2013 shows that a $-1.1(\pm0.7)\%\ yr^{-1}$ decrease in extinction can be attributed to decreasing aerosol water mass caused by the change in aerosol sulfate/organic ratio. Calculated reductions in extinction agree with regional trends in ground-based and satellite-derived aerosol optical depth. The diurnally averaged summertime surface radiative effect has changed by $8.0\ W\ m^{-2}$, with 19% attributed to the decrease in aerosol water.

1. Introduction

The 1990 Clean Air Act Amendments led to a 60% reduction in SO_2 emissions in the United States from 1990 to 2010 and reduced the mass concentration of $PM_{2.5}$ (particulate matter with aerodynamic diameters of less than 2.5 μm) sulfate (SO_4^{2-}) [*Hand et al.*, 2012a]. Sulfate aerosol affects direct and indirect aerosol radiative forcing, visibility, and health and typically reaches an annual peak in the summertime for most areas of the United States [*Hidy et al.*, 1978; *Poschl*, 2005; *Tai et al.*, 2010]. The fractional sulfate content of ambient particles directly affects their hygroscopicity. Particle size, complex refractive index, shape, and lifetime are a function of water content, and these properties determine the impact of aerosol on atmospheric visibility and the magnitude of direct radiative forcing of climate through changes in optical properties.

Decreases in SO_2 emissions have occurred concurrently with a $3.3\%\ yr^{-1}$ (1999–2010) decrease in emissions of anthropogenic volatile organic compounds (VOCs), which are precursors to secondary organic aerosol [*Spracklen et al.*, 2011; *Blanchard et al.*, 2013; *Hidy et al.*, 2014]. Anthropogenic VOC emission reductions are more difficult to quantify because they include a wider variety of sources and because methods for constructing inventories have changed over time. At least for certain sectors, VOC emissions have declined at rates comparable to those of other primary pollutants. For example, VOC emissions from mobile (on-road) sources decreased 63% from 1990 to 2010 and 44% from 2000 to 2010 in four southeastern states, including Alabama [*Blanchard et al.*, 2013] and $7.5\%\ yr^{-1}$ in the Los Angeles basin over the past five decades [*Warneke et al.*, 2012]. As a consequence of reduced SO_2 and VOC emissions, annual aerosol mass concentrations have decreased since 1990, especially in areas where sulfate is a dominant contributor [*Hidy et al.*, 2014]. Between 1992 and 2011, the calculated aerosol optical extinction decreased by 52% during the haziest 20% of days in the eastern U.S. [*Hand et al.*, 2014].

The Southern Oxidant and Aerosol Study (SOAS) was a large-scale, ground-based field intensive in Centreville, Alabama, during summer 2013, with multiple research objectives, including investigation of the impact of

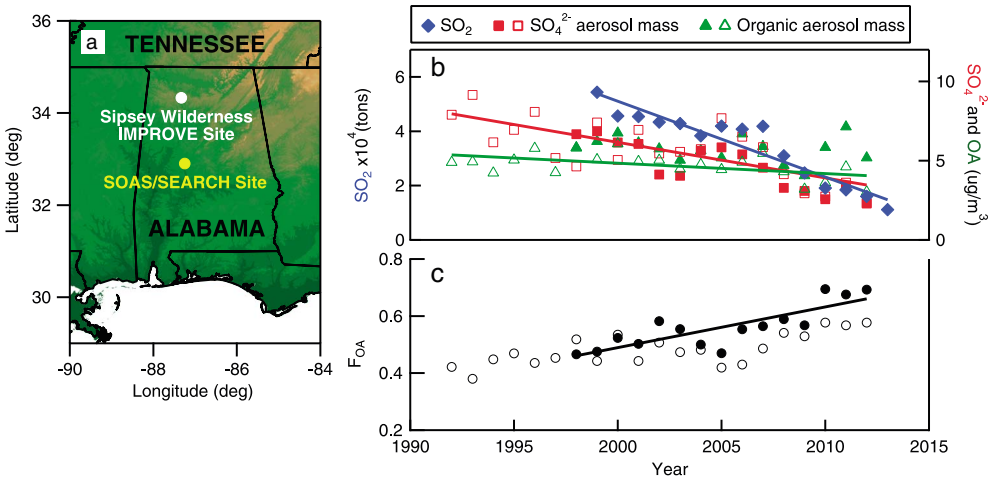

Figure 1. Long-term trends analysis for the Southeastern U.S. (a) Map of the Southeastern U.S. region showing the location of the SOAS/SEARCH Centreville field site and the Sipsey Wilderness IMPROVE site; (b) SO_2 emissions (statewide JJA average; left axis), SO_4^{2-}, and organic aerosol mass (organic carbon mass × 1.92) loading (JJA average; IMPROVE site open symbols, SEARCH site closed symbols; right axis) with overall trends for the IMPROVE sites (solid lines); and (c) corresponding annual F_{OA} and overall trend from the SEARCH data.

biogenic-anthropogenic interactions on regional climate and air quality. The aerosol composition in this region in recent years has been dominated by organics, which along with partially-neutralized ammonium sulfate compounds contribute 60–90% of surface $PM_{2.5}$ [*Edgerton et al.*, 2005; *Weber et al.*, 2007; *Hand et al.*, 2012b; *Zhang et al.*, 2012; *Hidy et al.*, 2014]. During summer in the Southeast U.S., about half of the measured organic carbon is thought to be produced by secondary formation mechanisms [*Lim and Turpin*, 2002].

During the SOAS field campaign, we deployed a novel, broadband cavity enhanced spectrometer (BBCES) to measure relative humidity (RH)-dependent aerosol extinction in the ultraviolet as a function of wavelength [*Washenfelder et al.*, 2013]. BBCES is a high-sensitivity measurement of optical extinction with continuous spectral resolution suitable for high precision, fast time response measurements of ambient aerosol optical properties. Here we report the RH dependence of aerosol extinction measured by the BBCES, along with speciated chemical composition data acquired during the SOAS field campaign. *Malm et al.* [2000] identified the important role of sulfate in determining aerosol hygroscopicity and suggested that controls on sulfur could dramatically improve visibility, especially in the eastern U.S. Here we demonstrate the dependence of aerosol hygroscopicity on aerosol composition for aerosol collected at a rural site in the Southeast U.S. that is consistent with this prediction and with prior analyses of aerosol hygroscopicity in other regions [*Quinn et al.*, 2004, 2005; *Doherty et al.*, 2005; *Massoli et al.*, 2009]. These findings show that recent decreases in aerosol sulfate relative to organics in the Southeastern U.S. have produced decreases in aerosol extinction, and its impacts on local climate forcing and visibility, due to decreased aerosol water. We combine the current measurements with regional trends in aerosol sulfate and organic mass from 1992 to 2013 to investigate how the effects of RH and changes in aerosol chemical composition have influenced local direct aerosol radiative forcing and visibility.

2. Method

2.1. Southern Oxidant and Aerosol Study

The SOAS 2013 ground site was located near Centreville, Alabama, at the existing Electric Power Research Institute Southeastern Aerosol Research and Characterization (SEARCH) network site (32°54′11.81″, 87° 14″59.79″W, 139 m above mean sea level), as shown in Figure 1a. Measurements were conducted between 1 June and 15 July 2013. The site is a rural, forested area within the Talladega National Forest, with isoprene emissions that are similar to those across the Southeastern U.S. [*Guenther et al.*, 2006]. Spectrally resolved aerosol extinction was measured by a novel broadband cavity enhanced spectrometer (BBCES), which provides a rapid, high-sensitivity measurement of optical extinction by ambient aerosol [*Washenfelder et al.*, 2013]. Each of the two BBCES channels consists of a light-emitting diode, collimating lens, optical cavity with

high-reflectivity mirrors, collection optics, and optical fiber bundle connected to a grating spectrometer with charge-coupled device (CCD) detector. The two BBCES channels together cover a wavelength range from 355 to 420 nm. Mirror reflectivity for the two broadband channels was determined every 30 min by measuring the extinction difference between helium and zero air (i.e., compressed air that has been scrubbed of potential absorbing gases), which have well known and large differences in Rayleigh scattering cross sections that vary smoothly with wavelength in the region of interest [*Washenfelder et al*., 2008, 2013]. Aerosol optical extinction was simultaneously measured with cavity ring-down spectroscopy (CRDS) using a diode laser at 403.2 nm.

The optical system and electronics were housed inside a temperature-controlled trailer. The two BBCES channels and CRDS channel drew a total flow at 6.0 standard liters per minute (sLpm) through a copper inlet (0.79 cm ID) located 6 m above ground, which was equally split into 2.0 sLpm flows for each channel. An additional 0.28 sLpm was sampled by a condensation particle counter (CPC; 3022A, TSI Inc., Shoreview, MN, USA) that continually measured particle number concentration. Prior to entering the CRDS sample cells and CPC, the flow passed through two nafion driers (PP-110-12-MSS, Perma Pure, Toms River, NJ) in parallel, decreasing the RH to <10%, an inertial impactor (TE296, Tisch Environmental, Cleves, OH) with a 50% cut point at 2.5 μm and a scrubber to remove NO_x ($NO_2 + NO$) and HONO. Both NO_2 and HONO have structured, gas phase absorption that can interfere with retrieval of aerosol extinction. The median aerosol diameter determined by a scanning mobility particle sizer during the SOAS field campaign was around 120 nm, and we assume that there is little contribution to extinction by particles greater than the instrument cut point. The sample flow alternated between <10% and 80% RH every 8 min to measure the humidity dependence of extinction. The 80% RH was achieved using a custom-built, temperature-controlled humidifier made with Accurel (Membrana, Wuppertal, Germany) water-permeable tubing. Temperature and RH were monitored immediately downstream of the CRDS sample cells. Measured aerosol extinction (α_{ext}) was averaged over 1 min intervals and corrected for measured particle loss in the humidifier (~3%).

Aerosol extinction as a function of RH is often parameterized using an empirical one-parameter power law fit:

$$\alpha_{ext}(RH) = \alpha_{ext}(RH_{ref}) \times \left[\frac{(100 - RH)}{(100 - RH_{ref})}\right]^{-\gamma_{ext}}, \quad (1)$$

where RH_{ref} is <10% RH and γ_{ext} increases with increased extinction due to water uptake onto the particle [*Hanel*, 1976; *Gassó et al*., 2000; *Zhou et al*., 2001; *Quinn et al*., 2005; *Massoli et al*., 2009]. The fraction of aerosol organic mass (F_{OA}) in submicron aerosols was calculated using the aerosol chemical composition data measured by a high-resolution time-of-flight aerosol mass spectrometer (AMS) during the SOAS field campaign. The AMS reports the mass of nonrefractory submicron aerosol species, including NH_4^+, SO_4^{2-}, NO_3^-, and organic aerosol (OA) and has been described previously [*DeCarlo et al*., 2006; *Canagaratna et al*., 2007]. The SO_4^{2-} and organic mass concentrations were used to calculate F_{OA}:

$$F_{OA} = \frac{m_{organic}}{m_{organic} + m_{sulfate}} \quad (2)$$

where $m_{organic}$ and $m_{sulfate}$ are the aerosol mass concentration of organic and sulfate. Sulfate is used as a proxy for all inorganic aerosol components because it is the largest contributor to inorganic mass and because the ratio in equation (2) has been used for prior analyses of the RH dependence of aerosol extinction [*Quinn et al*., 2005; *Massoli et al*., 2009].

2.2. Aerosol Composition From Ground Monitoring Sites in the Southeastern U.S.

The SEARCH network was established in 1998 for the long-term measurement of aerosol, gas, and meteorological data at four urban-rural site pairs [*Hansen et al*., 2003]. Besides continuous measurement of basic meteorology, gaseous air pollutants, $PM_{2.5}$ mass, and composition, 24 h integrated filters are analyzed for $PM_{2.5}$ mass, water-soluble ions, and trace elements. Historical data from the Centreville SEARCH site, which is collocated with the SOAS field site (Figure 1a), were used in this analysis. Additional speciated aerosol chemical mass data were obtained through the Interagency Monitoring of Protected Visual Environments (IMPROVE) monitoring network at the Sipsey Wilderness site located in northwestern Alabama [*Malm et al*., 1994], also shown in Figure 1a. The IMPROVE network was established in 1987 and currently operates more than 160 sites across the United States. Twenty-four hour filters were collected every three days and

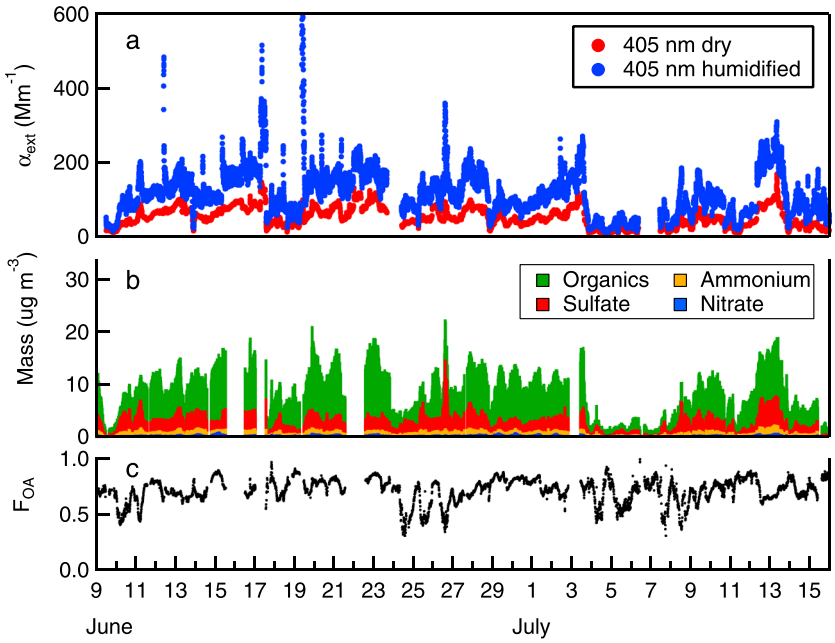

Figure 2. Aerosol extinction and composition measured during the SOAS field campaign. (a) Dry (RH < 10%) and humidified (RH = 80%) aerosol extinction (α_{ext}) measured by the BBCES at 405 nm, (b) aerosol mass loadings measured by the AMS for the entire SOAS field campaign, and (c) calculated fraction of organic aerosol mass (F_{OA}).

analyzed for the chemical components of $PM_{2.5}$. IMPROVE data were included due to their longer historical record and to examine an additional rural site in Alabama. For the historical data, we calculated aerosol organic mass by multiplying the reported aerosol organic carbon mass by 1.92 [*Philip et al.*, 2014]. Technical details for organic carbon sampling and intercomparison of the two networks have been described previously [*Chow et al.*, 2010; *Hand et al.*, 2013].

2.3. Historical SO_2 Emissions Data

Summertime SO_2 emission data from Alabama were retrieved from the Air Markets Program database maintained by the Environmental Protection Agency (http://ampd.epa.gov/ampd/). Complete emission data from all units were reported beginning in 2000, and we have examined the 2000–2013 period.

3. Results and Discussion

The long-term trend in summer (JJA) SO_2 emissions in Alabama from 2000 to 2013 from the Air Market Program database (see supporting information), along with trends in aerosol organic and sulfate mass from the IMPROVE Sipsey Wilderness site and SEARCH Centreville site, are shown in Figure 1b. During this period, summertime annual SO_2 decreased at a rate of $-9.5(\pm0.7)\%\ yr^{-1}$ and aerosol organic and sulfate mass decreased, with aerosol organics decreasing at an average rate of $-1.5(\pm0.6)\%\ yr^{-1}$ and $-0.9(\pm0.9)\%\ yr^{-1}$ and aerosol sulfate decreasing at an average rate of $-4.5(\pm0.9)\%\ yr^{-1}$ and $-6.8(\pm1.1)\%\ yr^{-1}$, as calculated from the IMPROVE (1992–2013) and SEARCH (1998–2013) data, respectively. The summertime-averaged F_{OA} increased over time at both sites due to the greater decrease in sulfate mass relative to organic mass (Figure 1c). Disagreement in F_{OA} between the two data sets arises from a higher concentration of organics measured at the SEARCH site, which has been reported previously and may represent methodological as well as local airshed differences [*Ford and Heald*, 2013].

Dry and humidified aerosol optical extinction coefficients measured during SOAS by BBCES at 405 nm are shown in Figure 2a. Dry extinction ranged from 6 to 180 Mm^{-1}, with lower aerosol mass and extinction after rain events. The aerosol was hygroscopic, and aerosol water enhanced extinction by an average factor of 1.5 at 80% RH. Extinction was measured from 355 to 420 nm and showed no detectable wavelength dependence in the enhancement at elevated RH. The nonrefractory aerosol chemical composition as

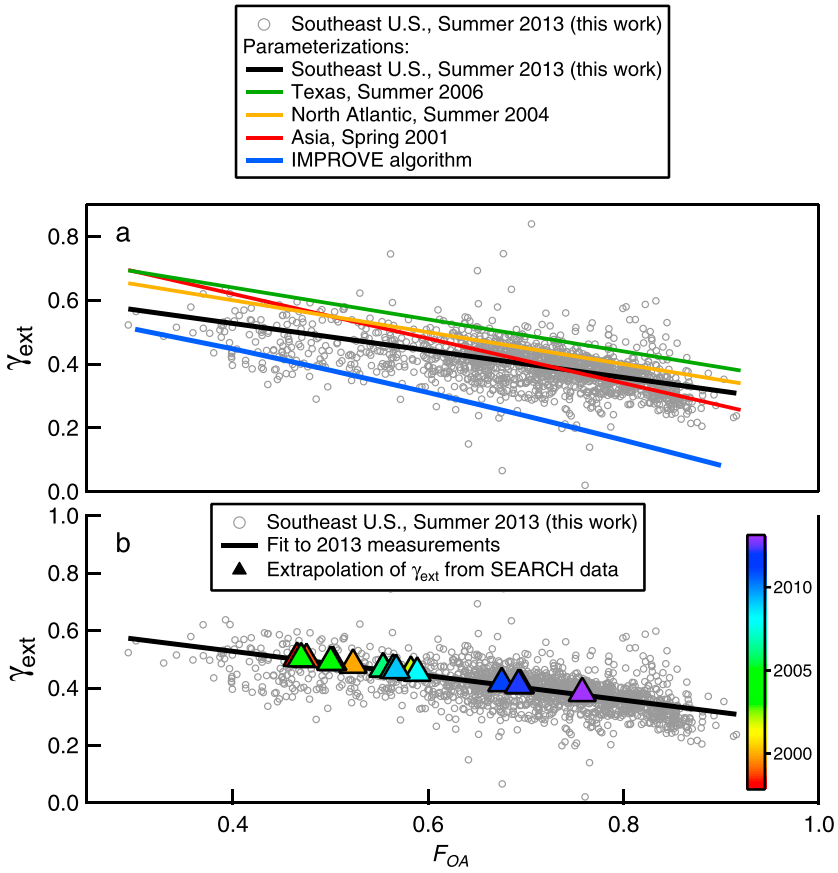

Figure 3. (a) The linear fit of γ_{ext} versus F_{OA} (black line) for the SOAS data (open grey circles), as well as three other field campaigns shown in solid lines and described in the text. (b) γ_{ext} versus F_{OA} for SOAS data as shown in Figure 3a but with calculated γ_{ext} from 1998 to 2013 using historical SEARCH F_{OA} data from Figure 1c.

measured by an AMS [*Canagaratna et al.*, 2007; *Jimenez et al.*, 2009] indicates that the aerosol sampled during SOAS was dominated by sulfate and organic mass (Figure 2b) but had variable F_{OA} (Figure 2c; average $F_{OA} = 0.7(\pm 0.1)$).

The enhancement in extinction with RH can be represented by a power law relationship (equation (1)) with an exponent, γ_{ext}. Previous studies have developed a linear parameterization that quantitatively describes the relationship between the hygroscopicity, γ_{ext}, and F_{OA} for use in radiative transfer and air quality models [*Quinn et al.*, 2005; *Massoli et al.*, 2009]. This correlation for the SOAS field campaign for aerosol optical extinction at 405 nm is shown in Figure 3a. This parameterization neglects the potential dependence of F_{OA} and hygroscopicity on aerosol size. The average SOAS F_{OA} determined by the AMS varied from 0.89 at mobility diameter 100 nm to 0.70 at mobility diameter 300 nm. However, the average surface area-weighted F_{OA} was 0.74, which was similar to the total mass F_{OA} of 0.70. The linear relationship determined from an orthogonal distance regression fit is

$$\gamma_{ext} = 0.70(\pm 0.02) - 0.42(\pm 0.02) \times F_{OA}. \quad (3)$$

There is no significant difference in fit for wavelengths between 355 and 420 nm. The fit is similar to those obtained from ambient measurements in the North Atlantic [*Quinn et al.*, 2005], Asia [*Quinn et al.*, 2004; *Doherty et al.*, 2005], and Texas [*Massoli et al.*, 2009], as shown in Figure 3a and summarized in the supporting information. Previous γ_{ext} values were determined at 532 nm, and all but the Texas study used scattering measurements. Because wavelength dependence of the aerosol hygroscopicity parameter, γ_{ext}, is weak and extinction during SOAS was dominated by scattering, the differences due to wavelength and absorption are expected to be small. The parameterization for the SOAS data and the three other campaigns agree within the

measurement uncertainty, indicating that the relationship is robust and broadly applicable to systems dominated by sulfate and organic aerosols [*Quinn et al*., 2005]. A detailed, alternative parameterization for aerosol hygroscopic growth is used to model visibility from IMPROVE network measurements of particulate mass [*Pitchford et al*., 2007] and yields similar results (within 12%) for average conditions at SOAS (see supporting information). The IMPROVE fit deviates from the other parameterizations at high organic fractions, because it neglects water uptake by organics and potentially also because the IMPROVE *f*(RH) growth factors assume that sulfate is fully neutralized as ammonium sulfate. During SOAS, the ammonium neutralization factor $[NH_4^+]/(2\times[SO_4^{2-}]+[NO_3^-]+[Cl^-])$ was 0.7(±0.1), indicating that sulfate was not fully neutralized. All fits show a trend of increased water uptake and enhanced extinction with a decrease in F_{OA}. This dependence of aerosol water mass on relative composition suggests that increases in F_{OA} in the Southeastern U.S. (Figure 1c) should itself lead to decreases in ambient aerosol extinction and changes to local aerosol radiative forcing and visibility independently from any associated decrease in total dry aerosol mass loading.

We determine the change in historical aerosol extinction due to changes in composition-driven hygroscopicity by applying the relationship between F_{OA} and γ_{ext} from SOAS (equation (3)) to the annual JJA average F_{OA} calculated from the SEARCH data shown in Figure 1c. Figure 3b shows that the increase in the average organic mass fraction of the aerosol in this region has led to a decrease in average hygroscopicity and average γ_{ext}. The decrease in average γ_{ext} ($\gamma = 0.49$ in 2001 to $\gamma = 0.38$ in 2013) corresponds to a decrease of $-1.1(\pm0.7)\%\ yr^{-1}$ in ambient extinction using the averaged local noon RH measured for JJA each year. The trend in ambient extinction differs slightly if the average local noon RH from 2013 is used (72.5% RH; $-1.0(\pm0.2)\%\ yr^{-1}$) or the average local noon RH from 2001 to 2013 (65.7% RH; $-0.8\%(\pm0.2)\ yr^{-1}$).

Since the extinction efficiency of ambient aerosol depends on size, this calculation is valid if the size distribution has not changed significantly with changes in mass loading over the two decades of historical record. The absence of historical data on aerosol size distribution in the Southeastern U.S. prevents us from determining the trend in size and its effect on aerosol extinction. However, we can estimate bounds by assuming that either there were fewer particles of the same size or the same number of smaller particles. In the former case there is no size distribution effect on γ_{ext}. In the latter case a 13% decrease in mass would correspond to a 4% decrease in diameter. Using a typical size distribution measured during SOAS, the size change would cause an 8.1% increase in γ_{ext} and correspond to a maximum decrease of a $-1.5\%\ yr^{-1}$ in ambient extinction at 72.5% RH.

In addition to the change in aerosol optical extinction attributed to changing F_{OA} and aerosol water content, aerosol extinction also decreased due to the historical decline in dry aerosol mass. As noted above, an algorithm (equation (S1)) has been developed and adopted by the U.S. Environmental Protection Agency as the basis for tracking haze levels for visibility-protected areas and is described in detail in the supporting information [*Pitchford et al*., 2007; *Brewer and Moore*, 2009]. We use this equation to calculate dry aerosol extinction at 550 nm by setting the *f*(RH) terms to unity. The calculated change in aerosol extinction is proportional to the change in total aerosol mass and depends primarily on mass extinction efficiencies for the different aerosol species. The decrease in aerosol optical extinction attributable to decrease in the total dry mass of $PM_{2.5}$ is calculated as $-3.4(\pm1.2)\%\ yr^{-1}$ during 2001–2013. Thus, the total change in extinction calculated due to decreased aerosol water and dry aerosol mass is $-4.5(\pm1.4)\%\ yr^{-1}$ during this period.

The long-term reductions in SO_2 emissions, sulfate concentrations, and F_{OA} (Figure 1) should have a measurable effect on visibility, aerosol optical depth (AOD, a dimensionless measure of the integrated extinction over a vertical column), and radiative forcing in this region.

We analyzed historical visibility data from the Automated Weather Observing System (AWOS) for 1992–2013, as described in detail in the supporting information. Three sites were chosen based on their proximity to the SOAS site and the completeness of the data record. Summertime visibility improved by $1.4(\pm0.1)\%\ yr^{-1}$ and $0.6(\pm0.1)\%\ yr^{-1}$ between 1992–2013 and 2001– 2013, respectively, across the three sites. However, these values can only be considered as lower limits, because the maximum reported AWOS visibility is 16 km (equivalent to an extinction of $63\ Mm^{-1}$), and visibility on many days was greater than the maximum.

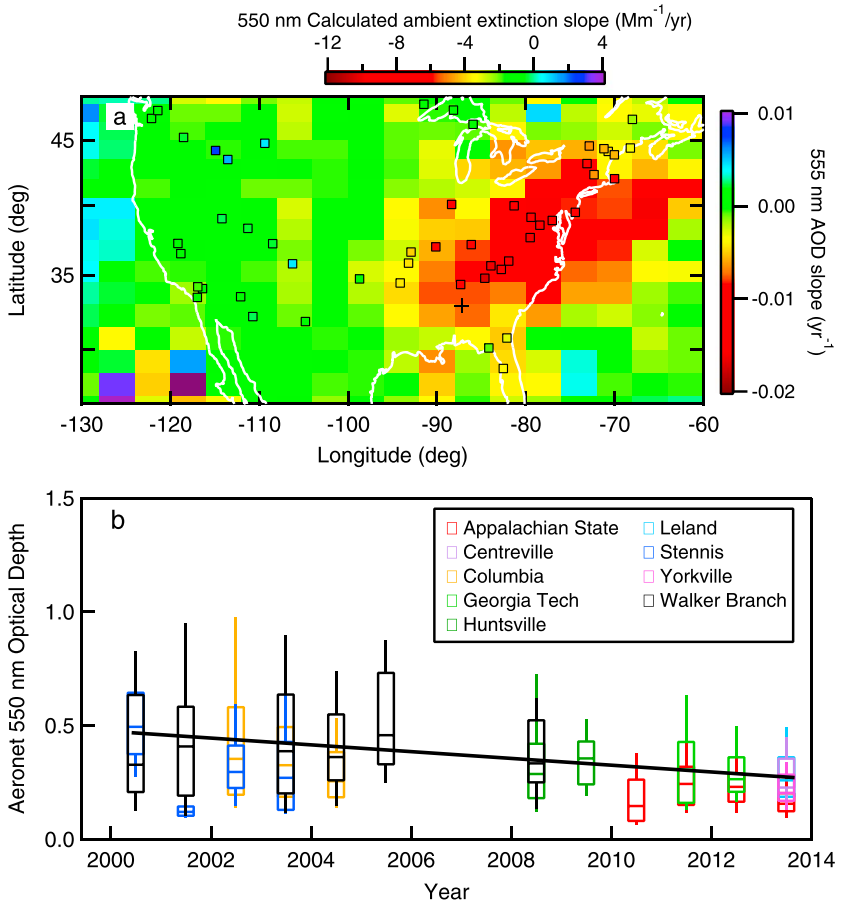

Figure 4. (a) Trends in aerosol optical depth (AOD) measured by the MISR satellite are shown with trends in calculated ambient extinction from the IMPROVE network (open squares). The SOAS field site is indicated (plus symbol). (b) Trends in AOD derived from AERONET data at 550 nm for nine temporally discontinuous sites during JJA in the Southeastern U.S. (see raw data, Figure S5).

The change in AOD for the continental U.S. during the summer (JJA) as measured by the Multiangle Imaging Spectroradiometer (MISR) satellite instrument from 2001 to 2013 at 555 nm [*Murphy*, 2013] is shown in Figure 4a along with the trend in ambient extinction from IMPROVE sites (calculated following *Pitchford et al*. [2007], with surface relative humidity from National Centers for Environmental Prediction surface relative humidity reanalysis data at 18 UTC. Within the 10° lat × 3° lon grid cell that contains the SOAS site, an average decrease of $-3.5\,\mathrm{yr}^{-1}$ in aerosol optical depth is calculated at 555 nm. We are unable to assign a trend uncertainty because the data are spatially autocorrelated so the data points are not independent.

Ground-based remote sensing Aerosol Robotic Network (AERONET) data collected from nine different stations across the Southeastern U.S. are shown in Figure 4b. An average decrease of $-4.1(\pm0.3)\%\ \mathrm{yr}^{-1}$ in AOD at 550 nm is calculated from 2001 to 2013. (Note that different AERONET stations operated during different years, potentially biasing this trend due to varying spatial coverage as a function of time; see supporting information.)

Both the satellite and ground-based remote sensing AOD values agree to within combined uncertainties with the calculated decrease of $-4.5(\pm1.4)\%\ \mathrm{yr}^{-1}$ in total extinction derived from the combined effects of reduced aerosol hygroscopicity and mass loading. While the absolute extinction at shorter wavelengths will be greater, the percentage trend will be similar at all wavelengths, assuming that Angstrom exponent has not significantly changed over time.

We calculated aerosol direct radiative forcing between 2001 and 2013 using the Santa Barbara discrete ordinates radiative transfer radiative transfer model [*Ricchiazzi et al*., 1998] to examine the effects of trends in extinction and hygroscopicity. Profiles for each year are constructed using the vertical distribution of RH and extinction derived from aircraft measurements over the SOAS site [*Langridge et al*., 2011] and the aerosol water mass from the previously described analyses. Calculations were made for an instantaneous forcing at solar noon on the summer solstice and for a diurnal average on the same day, both at the location of the Centreville site. For a median RH profile, a change in instantaneous (diurnally averaged) surface radiative forcing from −37.3 (−24.8) W m^{-2} in 2001 to −24.2 (−16.8) W m^{-2} in 2013 is found for the total changes in dry aerosol mass and aerosol water, with −2.2 (−1.5) W m^{-2} of that difference, or 17% (19%) of the total, due to the decrease in aerosol water alone (see supporting information for details on profiles and the comprehensive set of forcing calculations).

4. Conclusions

Reductions in U.S. SO_2 emissions that have led to changes in both dry aerosol mass and aerosol water mass are expected to continue in the future and may further reduce aerosol sulfate loading and mass fraction over the next decade. For example, the 2011 National Acid Precipitation Assessment [*Burns et al*., 2011] projects reduction in U.S. SO_2 emissions by a factor of 4–12.5 between 2009 and 2020. Alternatively, if the aerosol sulfate mass in the Southeastern U.S. continues to decrease at the same rate from 2009 to 2020 as it has during the recent period from 2009 to 2012 and the organic mass remains approximately constant, the resulting reduction in aerosol sulfate mass by a factor of 1.9 would produce a factor of 1.4 decrease in ambient aerosol extinction, more than a third of which would be due to aerosol water, driven by increases in F_{OA}. Globally, trends in SO_2 emissions vary by location, and understanding past and future changes in visibility or radiative forcing depends critically on uncertain trends in organic aerosol [*Jimenez et al*., 2009] since the change of sulfate relative to organic mass largely determines trends in hygroscopicity. For example, emissions of SO_2 in China increased by 91% from 1990 to 2005 and likely peaked in 2007 [*Smith et al*., 2011], but the trend in organic aerosol mass is unknown. The slower declines in organic aerosol relative to sulfate in the Southeastern U.S., despite large decreases in anthropogenic VOC emissions, may indicate an organic aerosol source dominated by oxidation of biogenic hydrocarbons or emissions from biomass burning. Relative sulfate and organic trends in other regions, especially those dominated by urban VOCs [*Warneke et al*., 2012], may differ substantially from those in the Southeastern U.S.

Acknowledgments

Data from the SOAS study are publicly available at http://www.esrl.noaa.gov/csd/projects/senex/. We acknowledge financial support from the NOAA Atmospheric Chemistry, Carbon Cycle and Climate Program (AC4). IMPROVE is a collaborative association of state, tribal, and federal agencies, and international partners; the U.S. Environmental Protection Agency is the primary funding source, with contracting and research support from the National Park Service; the Air Quality Group at the University of California, Davis, is the central analytical laboratory, with ion analysis provided by Research Triangle Institute and carbon analysis provided by Desert Research Institute. Funding for the SEARCH network is provided by Southern Company and the Electric Power Research Institute. The MISR data were obtained from the NASA Langley Research Center Atmospheric Science Data Center. We thank the following investigators for the effort in establishing and maintaining the AERONET sites used in this analysis: Brent N. Holben, James P. Sherman, Gary Gimmestad, Steve Tate, Brad Gingrey, and Kevin Knupp. The CU group acknowledges support from NSF AGS-1243354, NOAA NA13OAR4310063, and DOE (BER/ASR) DE-SC0011105.

Geoffrey Tyndall thanks two anonymous reviewers for their assistance in evaluating this paper.

References

Blanchard, C. L., G. M. Hidy, S. Tanenbaum, E. S. Edgerton, and B. E. Hartsell (2013), The Southeastern Aerosol Research and Characterization (SEARCH) study: Spatial variations and chemical climatology, 1999–2010, *J. Air Waste Manage.*, *63*(3), 260–275.

Brewer, P., and T. Moore (2009), Source contributions to visibility impairment in the southeastern and western United States, *J. Air Waste Manage.*, *59*(9), 1070–1081.

Burns, D. A., J. A. Lynch, B. J. Cosby, M. E. Fenn, and J. S. Baron (2011), *National Acid Precipitation Assessment Program Report to Congress 2011*, National Science and Technology Council, Washington, D. C.

Canagaratna, M. R., et al. (2007), Chemical and microphysical characterization of ambient aerosols with the aerodyne aerosol mass spectrometer, *Mass Spectrom. Rev.*, *26*(2), 185–222.

Chow, J. C., J. G. Watson, L. W. A. Chen, J. Rice, and N. H. Frank (2010), Quantification of PM2.5 organic carbon sampling artifacts in U.S. networks, *Atmos. Chem. Phys.*, *10*(12), 5223–5239.

DeCarlo, P. F., et al. (2006), Field-deployable, high-resolution, time-of-flight aerosol mass spectrometer, *Anal. Chem.*, *78*(24), 8281–8289.

Doherty, S. J., P. K. Quinn, A. Jefferson, C. M. Carrico, T. L. Anderson, and D. Hegg (2005), A comparison and summary of aerosol optical properties as observed in situ from aircraft, ship, and land during ACE-Asia, *J. Geophys. Res.*, *110*, D04201, doi:10.1029/2004JD004964.

Edgerton, E. S., B. E. Hartsell, R. D. Saylor, J. J. Jansen, D. A. Hansen, and G. M. Hidy (2005), The Southeastern Aerosol Research and Characterization Study: Part II. Filter-based measurements of fine and coarse particulate matter mass and composition, *J. Air Waste Manage.*, *55*(10), 1527–1542.

Ford, B., and C. L. Heald (2013), Aerosol loading in the Southeastern United States: Reconciling surface and satellite observations, *Atmos. Chem. Phys.*, *13*(18), 9269–9283.

Gassó, S., et al. (2000), Influence of humidity on the aerosol scattering coefficient and its effect on the upwelling radiance during ACE-2, *Tellus, Ser. B*, *52*(2), 546–567.

Guenther, A., T. Karl, P. Harley, C. Wiedinmyer, P. I. Palmer, and C. Geron (2006), Estimates of global terrestrial isoprene emissions using MEGAN (Model of Emissions of Gases and Aerosols from Nature), *Atmos. Chem. Phys.*, *6*(11), 3181–3210.

Hand, J. L., B. A. Schichtel, W. C. Malm, and M. L. Pitchford (2012a), Particulate sulfate ion concentration and SO_2 emission trends in the United States from the early 1990's through 2010, *Atmos. Chem. Phys.*, *12*(21), 10,353–10,365.

Hand, J. L., B. A. Schichtel, M. Pitchford, W. C. Malm, and N. H. Frank (2012b), Seasonal composition of remote and urban fine particulate matter in the United States, *J. Geophys. Res.*, *117*, D05209, doi:10.1029/2011JD017122.

Hand, J. L., B. A. Schichtel, W. C. Malm, and N. H. Frank (2013), Spatial and temporal trends in PM2.5 organic and elemental carbon across the United States, *Adv. Meteorol.*, *2013*, 367674, doi:10.1155/2013/367674.

Hand, J. L., B. A. Schichtel, W. C. Malm, S. Copeland, J. V. Molenar, N. Frank, and M. Pitchford (2014), Widespread reductions in haze across the United States from the early 1990s through 2011, *Atmos. Environ.*, *94*, 671–679.

Hanel, G. (1976), The properties of atmospheric aerosol particles as functions of the relative humidity at thermodynamic equilibrium with the surrounding moist air, *Adv. Geophys.*, *19*, 73–188.

Hansen, D. A., E. S. Edgerton, B. E. Hartsell, J. J. Jansen, N. Kandasamy, G. M. Hidy, and C. L. Blanchard (2003), The southeastern aerosol research and characterization study: Part 1—Overview, *J. Air Waste Manage.*, *53*(12), 1460–1471.

Hidy, G. M., P. K. Mueller, and E. Y. Tong (1978), Spatial and temporal distributions of airborne sulfate in parts of United States, *Atmos. Environ.*, *12*(1–3), 735–752.

Hidy, G. M., C. L. Blanchard, K. Baumann, E. Edgerton, S. Tanenbaum, S. Shaw, E. Knipping, I. Tombach, J. Jansen, and J. Walters (2014), Chemical climatology of the southeastern United States, 1999–2013, *Atmos. Chem. Phys. Discuss.*, *14*(11), 17,101–17,159.

Jimenez, J. L., et al. (2009), Evolution of organic aerosols in the atmosphere, *Science*, *326*(5959), 1525–1529.

Langridge, J. M., M. S. Richardson, D. Lack, D. Law, and D. M. Murphy (2011), Aircraft instrument for comprehensive characterization of aerosol optical properties, part I: Wavelength-dependent optical extinction and its relative humidity dependence measured using cavity ringdown spectroscopy, *Aerosol Sci. Technol.*, *45*(11), 1305–1318.

Lim, H.-J., and B. J. Turpin (2002), Origins of primary and secondary organic aerosol in Atlanta: Results of time-resolved measurements during the Atlanta Supersite Experiment, *Environ. Sci. Technol.*, *36*(21), 4489–4496.

Malm, W. C., J. F. Sisler, D. Huffman, R. A. Eldred, and T. A. Cahill (1994), Spatial and seasonal trends in particle concentration and optical extinction in the United States, *J. Geophys. Res.*, *99*(D1), 1347–1370, doi:10.1029/93JD02916.

Malm, W. C., D. E. Day, and S. M. Kreidenweis (2000), Light scattering characteristics of aerosols as a function of relative humidity: Part I—A comparison of measured scattering and aerosol concentrations using the theoretical models, *J. Air Waste Manage.*, *50*(5), 686–700.

Massoli, P., T. S. Bates, P. K. Quinn, D. A. Lack, T. Baynard, B. M. Lerner, S. C. Tucker, J. Brioude, A. Stohl, and E. J. Williams (2009), Aerosol optical and hygroscopic properties during TexAQS-GoMACCS 2006 and their impact on aerosol direct radiative forcing, *J. Geophys. Res.*, *114*, D00F07, doi:10.1029/2008JD011604.

Murphy, D. M. (2013), Little net clear-sky radiative forcing from recent regional redistribution of aerosols, *Nat. Geosci.*, *6*(4), 258–262.

Philip, S., et al. (2014), Spatially and seasonally resolved estimate of the ratio of organic mass to organic carbon, *Atmos. Environ.*, *87*, 34–40.

Pitchford, M., W. Malm, B. Schichtel, N. Kumar, D. Lowenthal, and J. Hand (2007), Revised algorithm for estimating light extinction from IMPROVE particle speciation data, *J. Air Waste Manage.*, *57*(11), 1326–1336.

Poschl, U. (2005), Atmospheric aerosols: Composition, transformation, climate and health effects, *Angew. Chem., Int. Ed.*, *44*(46), 7520–7540.

Quinn, P. K., et al. (2004), Aerosol optical properties measured on board the Ronald H. Brown during ACE-Asia as a function of aerosol chemical composition and source region, *J. Geophys. Res.*, *109*, D19S01, doi:10.1029/2003JD004010.

Quinn, P. K., et al. (2005), Impact of particulate organic matter on the relative humidity dependence of light scattering: A simplified parameterization, *Geophys. Res. Lett.*, *32*, L22809, doi:10.1029/2005GL024322.

Ricchiazzi, P., S. R. Yang, C. Gautier, and D. Sowle (1998), SBDART: A research and teaching software tool for plane-parallel radiative transfer in the Earth's atmosphere, *Bull. Am. Meteorol. Soc.*, *79*(10), 2101–2114.

Smith, S. J., J. van Aardenne, Z. Klimont, R. J. Andres, A. Volke, and S. Delgado Arias (2011), Anthropogenic sulfur dioxide emissions: 1850–2005, *Atmos. Chem. Phys.*, *11*, 1101–1116.

Spracklen, D. V., et al. (2011), Aerosol mass spectrometer constraint on the global secondary organic aerosol budget, *Atmos. Chem. Phys.*, *11*(23), 12,109–12,136.

Tai, A. P. K., L. J. Mickley, and D. J. Jacob (2010), Correlations between fine particulate matter ($PM_{2.5}$) and meteorological variables in the United States: Implications for the sensitivity of $PM_{2.5}$ to climate change, *Atmos. Environ.*, *44*(32), 3976–3984.

Thalman, R., K. J. Zarzana, M. A. Tolbert, and R. Volkamer (2014), Rayleigh scattering cross-section measurements of nitrogen, argon, oxygen and air, *J. Quant. Spectrosc. Radiat. Transfer*, *147*, 171–177.

Warneke, C., J. A. de Gouw, J. S. Holloway, J. Peischl, T. B. Ryerson, E. Atlas, D. Blake, M. Trainer, and D. D. Parrish (2012), Multiyear trends in volatile organic compounds in Los Angeles, California: Five decades of decreasing emissions, *J. Geophys. Res.*, *117*, D00V17, doi:10.1029/2012JD017899.

Washenfelder, R. A., A. O. Langford, H. Fuchs, and S. S. Brown (2008), Measurement of glyoxal using an incoherent broadband cavity enhanced absorption spectrometer, *Atmos. Chem. Phys.*, *8*(24), 7779–7793.

Washenfelder, R. A., J. M. Flores, C. A. Brock, S. S. Brown, and Y. Rudich (2013), Broadband measurements of aerosol extinction in the ultraviolet spectral region, *Atmos. Meas. Tech.*, *6*(4), 861–877.

Weber, R. J., et al. (2007), A study of secondary organic aerosol formation in the anthropogenic-influenced southeastern United States, *J. Geophys. Res.*, *112*, D13302, doi:10.1029/2007JD008408.

Zhang, X., Z. Liu, A. Hecobian, M. Zheng, N. H. Frank, E. S. Edgerton, and R. J. Weber (2012), Spatial and seasonal variations of fine particle water-soluble organic carbon (WSOC) over the southeastern United States: Implications for secondary organic aerosol formation, *Atmos. Chem. Phys.*, *12*(14), 6593–6607.

Zhou, J. C., E. Swietlicki, O. H. Berg, P. P. Aalto, K. Hameri, E. D. Nilsson, and C. Leck (2001), Hygroscopic properties of aerosol particles over the central Arctic Ocean during summer, *J. Geophys. Res.*, *106*(D23), 32,111–32,123, doi:10.1029/2000JD900426.